

Synthesis and Biophysical Studies of Coronene Functionalized 2'-Amino-LNA: A Novel Class of Fluorescent Nucleic Acids

Pankaj Gupta, Niels Langkjær, and Jesper Wengel*

Nucleic Acid Center, Department of Physics and Chemistry, University of Southern Denmark, 5230 Odense M, Denmark.

Received September 23, 2009; Revised Manuscript Received December 27, 2009

Incorporation of 2'-*N*-(coronen-1-yl)methyl-2'-amino-LNA monomer **X** or 2'-*N*-4-(coronen-1-yl)-4-oxobutanoyl-2'-amino-LNA monomer **Y** into short DNA strands induces high binding affinity toward DNA or RNA and a marked red-shift in steady-state fluorescence emission upon hybridization to cDNA or RNA.

INTRODUCTION

Fluorescent labeling of nucleosides and oligonucleotides is explored for structural studies, nucleic acid sequencing, molecular diagnostics, and other applications relating to genomics (1). "Molecular beacons" (2–4), fluorophore–quencher combination probes (5), "scorpion" (6), "Pacman" (7) or "sunrise primers," (8) specific pyrene-conjugated DNA or RNA probes (9–24), and fluorescence resonance energy transfer (FRET) probes (5, 25, 26) are typical example of such probes. Other fluorescent probes have been designed by labeling of oligonucleotides with a single hybridization sensitive moiety (17, 27–37). These methods have several potential advantages such as sensitivity, flexibility, safety, and relative inexpensiveness compared to the classical radiolabeling method.

The high-affinity hybridization of LNA (locked nucleic acid) (37–42), 2'-amino-LNA (43–45), and α -L-LNA (46) and the properties of LNA modified oligonucleotides as diagnostic tools and therapeutic agents (47, 48) encouraged us to appraise *N*-functionalized derivatives of 2'-amino-LNA. Recently, LNAs have been functionalized by fluorescent groups such as pyrene (15, 18, 49, 50), perylene (51, 52), and (phenylethynyl)pyrene (53). These pyrene-functionalized LNAs exhibit appealing properties and can be used to sense full complementarity of DNA or RNA counterparts.

Recently, Hrdlicka et al. (18) investigated multilabeled pyrene-functionalized 2'-amino-LNA probes which exhibited high-affinity hybridization to DNA/RNA complements, quenched fluorescence of single-stranded probe, and large increase of the quantum yield and fluorescence brightness upon hybridization. More recently, Astakhova et al. (52, 53) reported multilabeled perylene- and (phenylethynyl)pyrenecarbonyl-functionalized 2'-amino-LNA probes which exhibited high-affinity hybridization toward cDNA/RNA, considerably quenched fluorescence of single-stranded multilabeled probes, increased fluorescence brightness upon hybridization, high fluorescence quantum yields, and red-shifted emission compared to pyrene-functionalized 2'-amino-LNA probes. However, there is still a need to find optimal fluorochromes which, e.g., display a long-wave emission spectrum relative to pyrene, perylene, and (phenylethynyl)pyrenecarbonyl.

Coronene is a fluorochrome which resembles pyrene in its chemical behavior but differentiates from pyrene with respect to photochemical properties (54). Coronene is very stable, showing the properties of a fully benzenoid hydrocarbon. The extra stability of coronene imparted by the sextet ring current has been called "superaromaticity". Unlike pyrene, coronene is

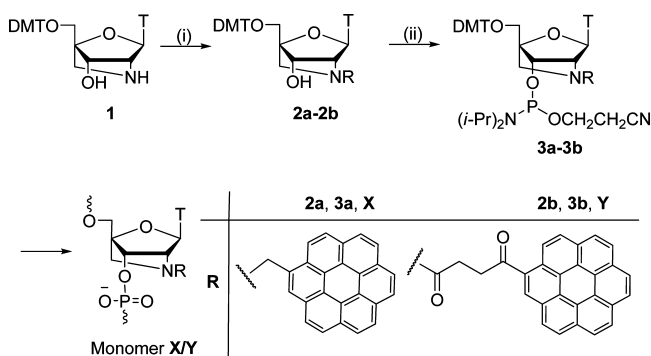
not a common fluorescent dye for modification of oligonucleotides, whereas it has been used in the field of lipids (55). Nagata et al. (56) described coronene as an external binder of DNA, but later, Zinger et al. (57) described that the planner coronene molecules partially insert between adjacent DNA bases. Herein, we report the synthesis of monomer **X** (with a methylcoronene moiety attached to 2'-amino-LNA) and monomer **Y** (with a oxobutanoylcoronene moiety attached to 2'-amino-LNA) and oligonucleotides involving them, together with their hybridization and fluorescence properties.

EXPERIMENTAL PROCEDURES

General. Anhydrous reactions were carried out under an atmosphere of nitrogen. Solvents used were of HPLC grade. Acetonitrile and dichloromethane were made anhydrous by storage over molecular sieves (4 Å). TLC was run with Merck silica 60 F₂₅₄ aluminum sheets. ¹H NMR spectra were recorded at 300 MHz, ¹³C NMR spectra at 75.5 MHz, and ³¹P NMR spectra at 121.5 MHz (δ H: CDCl₃ 7.26 ppm, DMSO-*d*₆ 2.50; δ C: CDCl₃ 77.0 ppm, DMSO-*d*₆ 39.4). Chemical shifts are reported in ppm relative to either tetramethylsilane or the deuterated solvent as an internal standard for ¹H NMR and ¹³C NMR, and relative to 85% H₃PO₄ as external standard for ³¹P NMR. Assignments of NMR spectra, when given, are based on 2D NMR experiments. Coupling constants (*J* values) are given in Hertz. ESI-HRMS were recorded in positive ion mode on an API QSTAR mass spectrometer.

Synthesis of ON2–ON10. Nucleoside phosphoramidites **3a** and **3b** were used as building blocks for incorporation of 2'-*N*-(coronen-1-yl)methyl-2'-amino-LNA monomer **X** and 2'-*N*-(coronen-1-yl)-4-oxo-butanoyl-2'-amino-LNA monomer **Y**, respectively, into DNA oligonucleotides (Scheme 1, Table 1) in 0.2 μ mol scale synthesis using an automated DNA synthesizer. Standard procedures were used for unmodified monomers (i.e., 3% trichloroacetic acid in CH₂Cl₂ as detritylation reagent; 0.25 M 4,5-dicyanoimidazole (DCI) in CH₃CN as activator; acetic anhydride in THF as cap A solution; *N*-methylimidazole in THF as cap B solution; and 0.02 M iodine in H₂O/pyridine/THF as the oxidizing solution). The stepwise coupling yields were >99% for unmodified phosphoramidites (2 min coupling time) and for **3a** and **3b** 95% and 99% (10 min coupling time, 1*H*-tetrazole as activator), respectively, based on the absorbance of the dimethoxytrityl cation released after each coupling step. After deprotection and cleavage from solid support (32% aq ammonia, 55 °C, 12 h), the modified ONs were precipitated and repeatedly washed with ethanol, and their composition and purity (>80%) verified by MALDI-MS analysis and ion-exchange HPLC, respectively.

* E-mail jwe@ifk.sdu.dk.

Scheme 1^a

^a Reagents and conditions: (i) (**2a**) Coronene-1-carbaldehyde, NaBH(OAc)₃, ClCH₂CH₂Cl, rt, 60%; (**2b**) 4-(coronen-1-yl)-4-oxobutanoic acid, 1-ethyl-3-(3-dimethylaminopropyl)carbodiimide hydrochloride (EDC·HCl), CH₂Cl₂, 59%; (ii) bis(*N,N*-diisopropylamino)-2-cyanoethoxyphosphine, *N,N*-diisopropylammonium tetrazolide, MeCN/CH₂Cl₂ (5:2), 2 h for **3a**/35 °C, 3 h for **3b**/rt; **3a**, 80%; **3b**, 75%. T = thymine-1-yl. DMT = 4,4'-dimethoxytrityl.

Table 1. Thermal Denaturation Studies Towards DNA/RNA^a

oligonucleotides	DNA		RNA	
	<i>T_m</i> /°C	Δ <i>T_m</i> /°C	<i>T_m</i> /°C	Δ <i>T_m</i> /°C
ON1 5'-d(GTG ATA TGC) ^b	28.5	ref.	26.5	ref.
ON2 5'-d(GCA TAT CAC)	28.5	ref.	24.5	ref.
ON3 5'-d(GTG AXA TGC) ^{c,d}	31.5	+3.0	28.0	+1.5
ON4 5'-d(GCA TAX CAC)	27.0	-1.5	24.0	-0.5
ON5 5'-d(GCA XAT CAC)	30.5	+2.0	27.5	+3.0
ON6 5'-d(GCA XAX CAC)	17.5/36.5		18.0/37.0	
ON7 5'-d(GTG AYA TGC) ^{c,d}	43.0	+14.5	36.0	+9.5
ON8 5'-d(GCA TAY CAC)	37.5	+9.0	36.5	+12.0
ON9 5'-d(GCA YAT CAC)	43.5	+15.0	35.0	+10.5
ON10 5'-d(GCA YAY CAC)	31.5	+1.5	19.0	-2.7

^a Thermal denaturation temperatures [*T_m* values (°C) (Δ*T_m* = change in *T_m* value calculated relative to DNA/DNA or DNA/RNA reference duplex)] measured as the maximum of the first derivative of the melting curve (*A*₂₆₀ vs temperature) recorded in 10 mM phosphate buffer ([Na⁺] = 110 mM, [Cl⁻] = 100 mM, [EDTA] = 0.1 mM, pH 7.0) using 1.0 μM concentrations of the two complementary strands. *T_m* values are averages within ±1 °C of at least two measurements. See Scheme 1 for structure of monomer X and monomer Y. MALDI-MS *m/z* ([M-H]⁻; found/calc.): **ON3**, 3092/3093; **ON4**, 3020/3022; **ON5**, 3021/3022; **ON6**, 3360/3361; **ON7**, 3161/3163; **ON8**, 3088/3092; **ON9**, 3090/3092; **ON10**, 3500/3501. ^b **ON1** is the cDNA strand to **ON2/ON4/ON5/ON6/ON8/ON9/ON10**; **ON2** is the cDNA strand to **ON3/ON7**. ^c *T_m* values (°C) toward DNA strands containing a single mismatch in the central position, monomer X: G/C/T: 24.0/31.5/28.0; monomer Y: G/C/T: 36.5/30.0/35.5. ^d *T_m* values (°C) toward RNA strands containing a single mismatch in the central position, monomer X: G/C/U: 21.0/21.0/18.5; monomer Y: G/C/U: 30.0/17.0/22.0.

Thermal Denaturation Studies. Concentrations of oligonucleotides were calculated using the following extinction coefficients (OD/μmol): G, 10.5; A, 13.9; T/U, 7.9; C, 6.6; coronene units, 36.0. The two complementary strands (~1.0 μM) were thoroughly mixed, and the duplex denatured by heating to 80 °C followed by cooling to the starting temperature (5 °C) of the experiment. Quartz optical cells with a path length of 1.0 cm were used. Thermal denaturation curves were obtained on a Perkin-Elmer Lambda 35 UV/vis spectrometer equipped with a PTP-6 peltier temperature programmer. Melting temperatures (*T_m* values/°C) determined as the maximum of the first derivative of the thermal denaturation curve (*A*₂₆₀ vs temperature) recorded in 10 mM phosphate buffer ([Na⁺] = 110 mM, [Cl⁻] = 100 mM, [EDTA] = 0.1 mM, pH 7.0). A temperature range from 5 to 75 °C with a ramp of 1.0 °C/min was used.

UV Absorption Measurements. UV absorption measurements (200–500 nm) were performed on a Shimadzu UV-160A

spectrophotometer using quartz optical cells with a path length of 1.0 cm. Measurements were conducted using 1.0 μM of strands in 10 mM phosphate buffer ([Na⁺] = 110 mM, [Cl⁻] = 100 mM, [EDTA] = 0.1 mM, pH 7.0).

(**1R,3R,4R,7S**)-5-[4-Coronen-1-ylmethyl]-1-(4,4'-dimethoxytrityloxymethyl)-7-hydroxy-3-(thymine-1-yl)-2-oxa-5-azabicyclo[2.2.1]heptane (**2a**). Nucleoside **1** (**58**) (0.23 g, 0.40 mmol) was dissolved in anhydrous 1,2-dichloroethane (5 mL). To this stirred solution at rt were added coronene-1-carbaldehyde (0.14 g, 0.42 mmol) and sodium triacetoxyborohydride (0.12 g, 0.60 mmol). After stirring at rt for 6 h, saturated aq NaHCO₃ (2 mL) was added and the mixture diluted with ethylacetate (20 mL). The organic phase was washed with saturated aq NaHCO₃ (10 mL) and the aq phase was extracted with ethylacetate (2 × 20 mL). The combined organic phase was dried over Na₂SO₄, filtered, and evaporated to dryness under reduced pressure, and the resulting residue was purified by silica gel column chromatography (20–70% EtOAc in petroleum ether, v/v) to afford nucleoside **2a** as a yellowish solid material (210 mg; 60%). *R_f* = 0.35 (7% MeOH in CH₂Cl₂, v/v); ESI-HRMS *m/z* 906.3127 ([M+Na]⁺, C₅₇H₄₅N₃O₇·Na⁺ calc. 906.3149); ¹H NMR (DMSO-*d*₆) δ (selected signals) 11.39 (s, NH), 9.16–8.91 (m, Ar), 7.70 (s, H₆), 7.48–6.88 (m, Ar), 5.94 (s, 3'-OH), 5.74 (d, *J* = 6.0 Hz, H1'), 5.21 (d, *J* = 14.4 Hz, CH₂Ar), 5.03 (d, *J* = 14.7 Hz, CH₂Ar), 4.35 (d, *J* = 4.5 Hz, H2'), 3.78–3.72 (m, H3' and 2 × OCH₃), 3.48 (d, *J* = 10.8 Hz, H5'a/b), 3.38–3.35 (m, H5'a/b overlapping with H₂O), 3.18 (d, *J* = 9.6 Hz, H5''a), 2.97 (d, *J* = 6.0 Hz, H5''b), 1.55 (s, CH₃); ¹³C NMR (DMSO-*d*₆) δ 163.8, 158.1, 150.0, 144.7, 135.4, 135.2, 134.7, 134.0, 129.8, 129.7, 128.1, 128.0, 127.9, 127.8, 127.6, 126.9, 126.8, 126.3, 126.1, 126.0, 125.8, 122.6, 121.8, 121.6, 121.5, 121.3, 121.2, 120.8, 113.2, 108.2, 88.5, 86.2, 85.6, 70.7, 66.5, 59.7, 58.1, 56.8, 55.0, 12.4.

(**1R,3R,4R,7S**)-5-[4-Coronen-1-ylmethyl]-7-[2-cyanoethoxy-(diisopropylamino)-phosphinoxy]-1-(4,4'-dimethoxytrityloxymethyl)-3-(thymine-1-yl)-2-oxa-5-azabicyclo[2.2.1]heptane (**3a**). Nucleoside **2a** (0.13 g, 0.14 mmol) was dissolved in anhydrous acetonitrile (5 mL) under stirring at rt. *N,N*-Diisopropylammonium tetrazolide (0.037 g, 0.22 mmol) and bis(*N,N*-diisopropylamino)-2-cyanoethoxyphosphine (0.14 mmol, 0.44 mmol) were added under nitrogen. The reaction mixture was stirred for 3 h at 35 °C and then diluted with EtOAc (40 mL), washed with H₂O (30 mL), 5% aq NaHCO₃ (30 mL) and H₂O (30 mL), dried over Na₂SO₄, filtered, and evaporated to dryness under reduced pressure. The residue was purified by silica gel column chromatography (20–60% EtOAc in petroleum ether, v/v) to afford nucleoside **3a** as a yellowish solid material (118 mg; 74%). *R_f* = 0.60 (60% EtOAc in petroleum ether, v/v); ESI-HRMS *m/z* 1106.4259 ([M+Na]⁺, C₆₆H₆₂N₅O₈P·Na⁺ calc. 1106.4227); ³¹P NMR (CDCl₃) δ 149.1.

(**1R,3R,4R,7S**)-5-[4-(Coronen-1-yl)-4-oxo-butanoyl]-1-(4,4'-dimethoxytrityloxymethyl)-7-hydroxy-3-(thymine-1-yl)-2-oxa-5-azabicyclo[2.2.1]heptane (**2b**). Nucleoside **1** (**58**) (0.40 g, 0.69 mmol) was dissolved in anhydrous dichloromethane (20 mL). To this stirred solution were added *N*-(3-dimethylaminopropyl)-*N'*-ethylcarbodiimide hydrochloride (EDC·HCl, 0.14 g, 0.76 mmol) and 3-coronenyl propionic acid (0.30 g, 0.76 mmol) at 0 °C. After warming to rt, the reaction mixture was stirred for 18 h, whereupon it was diluted with dichloromethane (50 mL) and successively washed with brine (40 mL) and H₂O (40 mL). The organic phase was evaporated to dryness under reduced pressure, and the resulting residue was purified by silica gel column chromatography (0–2% MeOH in CH₂Cl₂, v/v) to afford a rotameric mixture (~1:0.43 by ¹H NMR) of **2b** as a yellowish solid material (380 mg; 58%). *R_f* = 0.32 (7% MeOH in CH₂Cl₂, v/v); ESI-HRMS *m/z* 976.3291 ([M+Na]⁺, C₆₀H₄₇N₃O₉·Na⁺ calc. 976.3210); ¹H NMR (DMSO-*d*₆) δ

(selected signals) 11.50 (br s, NHA), 11.35 (br s, NHB), 9.53–8.92 (m, Ar), 7.79 (s, H6), 7.63–6.82 (m, Ar), 5.68 (s, H-1'A), 5.52 (br s, H-1'B), 4.77 (br s, H-2'B), 4.63 (br s, H-2'A), 4.14 (br s, H-3'A and H-3'B), 1.83 (br s, CH₃-A), 1.16 (br s, CH₃-B); ¹³C NMR (DMSO-*d*₆) δ 203.6, 202.1, 170.7, 170.5, 164.0, 157.8, 150.1, 148.3, 140.2, 134.9, 134.9, 133.9, 132.1, 132.0, 129.2, 129.1, 128.9, 128.4, 128.3, 128.0, 127.9, 127.6, 127.4, 127.1, 126.9, 126.8, 126.6, 126.5, 126.4, 126.2, 126.0, 124.8, 124.0, 122.5, 121.9, 121.2, 121.1, 120.9, 120.7, 113.9, 112.7, 109.9, 108.3, 108.2, 89.4, 88.8, 86.4, 79.9, 68.4, 63.3, 56.6, 55.0, 54.9, 50.8, 45.6, 42.0, 36.9, 28.5, 12.4, 10.9.

(**1R,3R,4R,7S**)-5-[4-(Coronen-1-yl)-4-oxo-butanoyl]-7-[2-cyanoethoxy(diisopropylamino)phosphinoxy]-1-(4,4'-dimethoxytrityloxymethyl)-3-(thymine-1-yl)-2-oxa-5-azabicyclo[2.2.1]heptane (**3b**). Nucleoside **2b** (0.32 g, 0.33 mmol) was dissolved in a mixture of anhydrous acetonitrile (7.0 mL) and dichloromethane (2.0 mL) under stirring at rt. *N,N*-Diisopropylammonium tetrazolide (0.057 g, 0.50 mmol) and bis(*N,N*-diisopropylamino)-2-cyanoethoxyphosphine (0.31 mL, 1.00 mmol) were added under nitrogen. The reaction mixture was stirred for 2 h and then diluted with EtOAc (60 mL), washed successively with H₂O (40 mL), 5% aq NaHCO₃ (40 mL) and H₂O (40 mL), dried over Na₂SO₄, filtered, and evaporated to dryness under reduced pressure. The residue was purified by silica gel column chromatography (30–90% EtOAc in petroleum ether, v/v) to afford nucleoside **3b** as a yellowish solid material (300 mg; 79%). *R*_f = 0.60 (80% EtOAc in petroleum ether, v/v); ESI-HRMS *m/z* 1176.4282 ([M+Na]⁺, C₆₉H₆₄N₅O₁₀P·Na⁺ calc. 1176.4333); ³¹P NMR (CDCl₃) δ 149.0, 150.2.

RESULTS

The bicyclic nucleoside **1** was synthesized according to a published procedure (58) and was selectively *N*-alkylated by reductive amination using coronene-1-carbaldehyde producing *N*-(coronen-1-yl)methyl derivative **2a**. Furthermore, **1** was *N*-acylated by 4-(coronen-1-yl)-4-oxobutanoic acid giving the corresponding nucleoside **2b**. The phosphoramidite building blocks **3a** and **3b** were obtained by standard phosphitylation of nucleosides **2a** and **2b**, respectively, using bis(*N,N*-diisopropylamino)-2-cyanoethoxyphosphine as phosphitylating agent (Scheme 1).

Synthesis of oligonucleotides (ONs) containing 2'-amino-LNA monomers **X** and **Y** was performed in 0.2 μmol scale using an automated DNA synthesizer. 1*H*-Tetrazole was used as coupling agent for monomers **X** and **Y** resulting in 95% and 99% stepwise coupling yields, respectively, based on the absorbance of the dimethoxytrityl cation released after each coupling step (see Experimental Procedures section for details). All synthesized ONs were purified by RP-HPLC, and their identity was confirmed by MALDI-TOF mass spectroscopy and ion-exchange HPLC, respectively.

The influence of the functionalized 2'-amino-LNA monomers **X** and **Y** on duplex thermal stabilities was studied toward DNA and RNA complements (Table 1) by UV thermal denaturation experiments using a 10 mM phosphate buffer ([Na⁺] = 110 mM, [Cl⁻] = 100 mM, [EDTA] = 0.1 mM, pH 7.0). In all cases, the denaturation curves displayed monophasic transitions.

Earlier, it was reported that conjugates containing functionalized 2'-amino-LNA monomers form stable duplexes toward both DNA and RNA complements, and that *N*'-acylated 2'-amino-LNA derivatives exhibit higher thermal stabilities than the corresponding *N*'-alkylated derivatives (18, 49). Our results are in good agreement with these earlier results. Incorporation of a single monomer **X** in mixed 9-mer **ON3** and **ON5** induced an increase in duplex stability toward cDNA (Δ*T*_m = +2.0 and +3.0 °C compared to the unmodified reference duplex **ON1:ON2**) (Table 1). A similar effect was observed for **ON3** and

Table 2. Thermal Denaturation Studies in Zipper Arrangements^a

Duplexes	<i>T</i> _m /°C	Δ <i>T</i> _m /°C	Schematic illustration	Constitution
ON1 :5'-d(GTG ATA TGC) ON2 :3'-d(CAC TAT ACG)	28.5	Ref.		
ON3 :5'-d(GTG AXA TGC) ON4 :3'-d(CAC XAT ACG)	49.0	+20.5		-1 Zipper
ON3 :5'-d(GTG AXA TGC) ON5 :3'-d(CAC TAX ACG)	33.5	+5.0		+1 Zipper
ON7 :5'-d(GTG AYA TGC) ON8 :3'-d(CAC YAT ACG)	57.0	+28.5		-1 Zipper
ON7 :5'-d(GTG AYA TGC) ON9 :3'-d(CAC TAY ACG)	47.0	+18.5		+1 Zipper

^aThermal denaturation temperatures were recorded under the same conditions as described in Table 1. See Scheme 1 for structures of monomer **X** and monomer **Y**. The black droplets illustrate the coronene moieties of **X** and **Y** monomers.

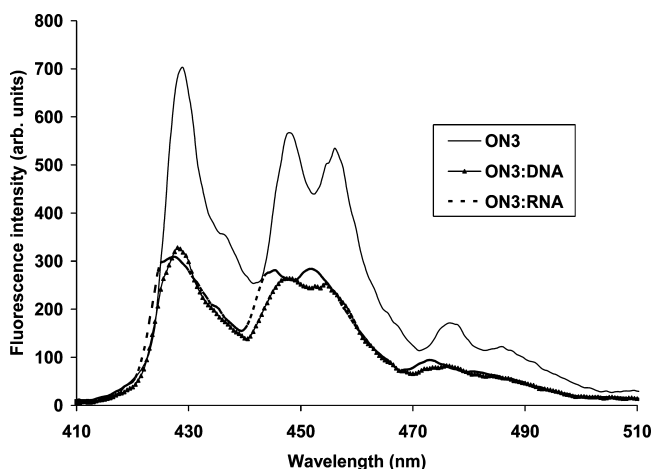


Figure 1. Steady-state fluorescence emission spectra of single-stranded probe **ON3** (with monomer **X**) and of duplexes formed between **ON3** and cDNA (**ON3:DNA**) or RNA (**ON3:RNA**).

ON5 with complementary RNA. Surprisingly, **ON4** showed minor destabilization toward cDNA (Δ*T*_m = -1.5 °C) and complementary RNA (Δ*T*_m = -0.5 °C). In contrast to the melting temperature results of monomer **X**, a single incorporation of monomer **Y** in mixed DNA 9-mer ONs (**ON7–ON9**) induced high-affinity hybridization toward DNA (Δ*T*_m = +9.0 to +15.0 °C) and RNA (Δ*T*_m = +9.5 to +12.0 °C). When comparing thermal stabilities of duplexes involving ONs singly functionalized with monomer **Y**, (**ON7–ON9**) were higher than those of the corresponding unmodified duplexes and of duplexes involving a perylenemethyl-2'-amino-LNA monomer (51), (phenylethynyl)pyrene-functionalized 2'-amino-LNAs (53) and *N*'-pyrenecarbonyl-functionalized 2'-amino-LNAs (18). This indicates that attachment of coronene moieties to 2'-amino-LNA monomers is compatible with duplex formation. To evaluate this further, we performed CD experiments on duplexes formed between **ON8** or **ON9**, each containing one **Y** monomer, and cDNA or RNA (S7, ESI). These spectra indicate similar duplex structures of the modified duplexes and the unmodified reference (**ON2:DNA** and **ON2:RNA**) duplexes, which support that one **Y** modification can be accommodated without significantly disturbing overall duplex structure.

Incorporation of two modifications may, however, have a more profound effect on duplex structure. *N*'-Substituents of 2'-amino-LNAs are known to point toward the minor groove (15, 49) and may therefore be affected by the narrow minor grooves in A-type duplexes (59). Incorporation of two **X** monomers separated by one nucleotide in a 9-mer DNA strand (**ON6**)

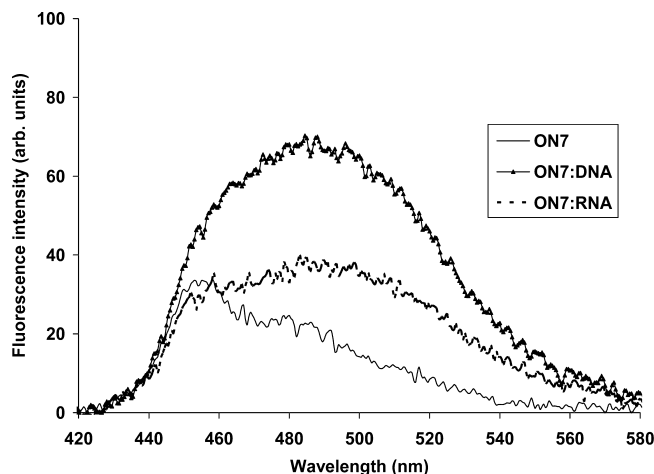


Figure 2. Steady-state fluorescence emission spectra of single-stranded probe ON7 (with monomer Y) and of duplexes formed between ON7 and cDNA (ON7:DNA) and RNA (ON7:RNA).

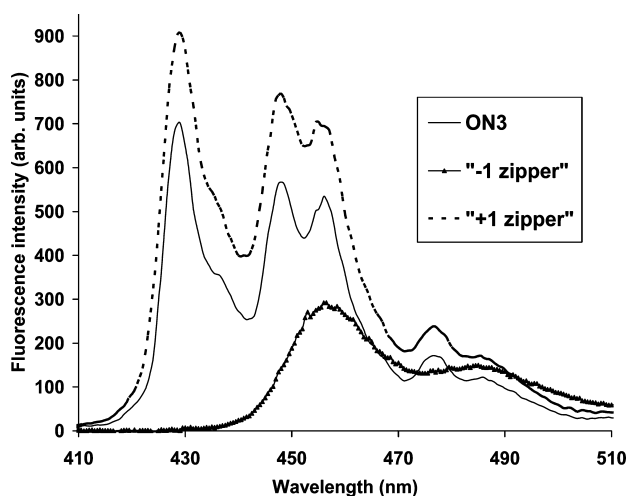


Figure 3. Steady-state fluorescence emission spectra of single-stranded probe ON3 (with monomer X) and of duplexes formed between ON3 and ON4 (“-1 zipper” constitution) and ON3 and ON5 (“+1 zipper” constitution).

resulted in two melting transitions, which we at present are unable to explain; no transition was observed for ON6 without a complementary strand. On the contrary, single transitions upon incorporation of two Y monomers separated by one nucleotide (ON10) were obtained with enhanced thermal stability of the duplex with cDNA ($\Delta T_m = +1.5$ °C per modification) but decreased thermal stability of the duplex with complementary RNA ($\Delta T_m = -2.7$ °C per modification). Relative destabilization toward DNA/RNA complements upon sequential incorporation of two monomers Y (relative to incorporation of one Y monomer) suggests that the minor groove is too narrow to accommodate the two coronene moieties.

The Watson–Crick base pair selectivity of monomers X and Y was evaluated by observing thermal denaturation temperatures of duplexes formed between ON3/ON7 and DNA or RNA strands containing a single mismatched nucleotide opposite monomer X or Y (see Table 1; footnotes c and d). The base pair selectivity of monomer X was satisfactory in the case of T:G DNA and T:U RNA mismatches (-7.5 °C/ -9.5 °C, respectively). A relatively weak decrease in thermal stability was observed for the T:T DNA mismatch (-3.5 °C), whereas no mismatch discrimination was observed for the T:C DNA mismatch. Against RNA, ON3 showed appreciable mismatch discrimination. The base pairing selectivity of monomer Y was

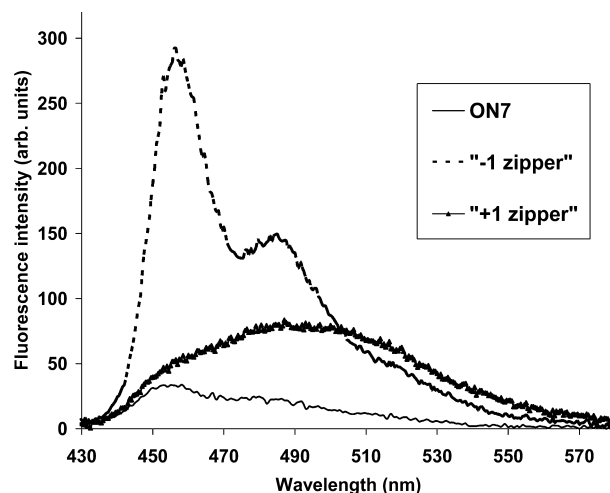


Figure 4. Steady-state fluorescence emission spectra of single-stranded probe ON7 (with monomer X) and of duplexes formed between ON7 and ON8 (“-1 zipper” constitution) and ON7 and ON9 (“+1 zipper” constitution).

satisfactory in both DNA and RNA contexts: T:T/U (-7.5 °C/ -14.0 °C, respectively), T:G (-6.5 °C/ -6.0 °C, respectively), and T:C (-13.0 °C/ -19.0 °C, respectively).

Studies with X/Y monomers positioned in both strands of a duplex were performed in -1 and +1 interstrand zipper (15) arrangements of monomer X or Y (Table 2). Insertion of two X monomers in a “-1 zipper” constitution induced extensively increased thermal stability (Table 2, $\Delta T_m = +20.5$ °C), as did insertion of two Y monomers ($+28.5$ °C). On the other hand, insertion of two X monomers in a “+1 zipper” constitution induced a limited increase in thermal stability ($+5.0$ °C), whereas insertion of two Y monomers in a “+1 zipper” constitution again induced a significant increase in thermal stability ($+18.5$ °C). The thermal denaturation temperatures of duplexes involving two modified strands are thus remarkably higher than those of duplexes containing monomers X or Y in only one strand, indicating that interstrand communication between coronene moieties in the studied “zipper” pattern contributes to overall duplex stability.

The steady-state fluorescence emission spectra of ON3–ON6 containing monomer X when excited at its UV absorption maximum λ_{max} 310 nm (10 °C, ± 1 °C) showed three emission bands. Insertion of a single X monomer in ONs (ON3–ON5) in general results in quenching of fluorescence intensities (up to half of the intensity of single-stranded ONs) upon hybridization to cDNA or RNA, though a minor increase of fluorescence intensity in the case of ON4 was observed upon hybridization to cDNA. (Figure 1, and ESI S4.1 to S4.4). However, ON6 with two X monomers separated by one nucleotide upon hybridization with cDNA displayed increased fluorescence intensity (~ 2 -fold) with unchanged emission wavelength and upon hybridization with complementary RNA slightly increased fluorescence intensity at nearly the same emission wavelength (see ESI S4.5). Incorporation of monomer X in ONs (ON3–ON6) results in fluorescence emission maxima at ~ 429 nm, which is 25 nm red-shifted relative to the corresponding pyrenecarbonyl-2'-amino-LNA ONs (18), 61 nm blue-shifted relative to the corresponding perylene-3-carbonyl-2'-amino-LNA ONs (52) and 1–26 nm blue-shifted relative to the corresponding (phenylethynyl)pyrenecarbonyl-2'-amino-LNA ONs (53).

In contrast, insertion of a single Y monomer into ONs (ON7–ON9) in general results in a marked red shift with similar or increased fluorescence intensities upon hybridization to cDNA or RNA (Figure 2 and ESI, S4.6 to S4.9). Surprisingly, ON10 containing two Y monomers upon duplex formation with DNA/

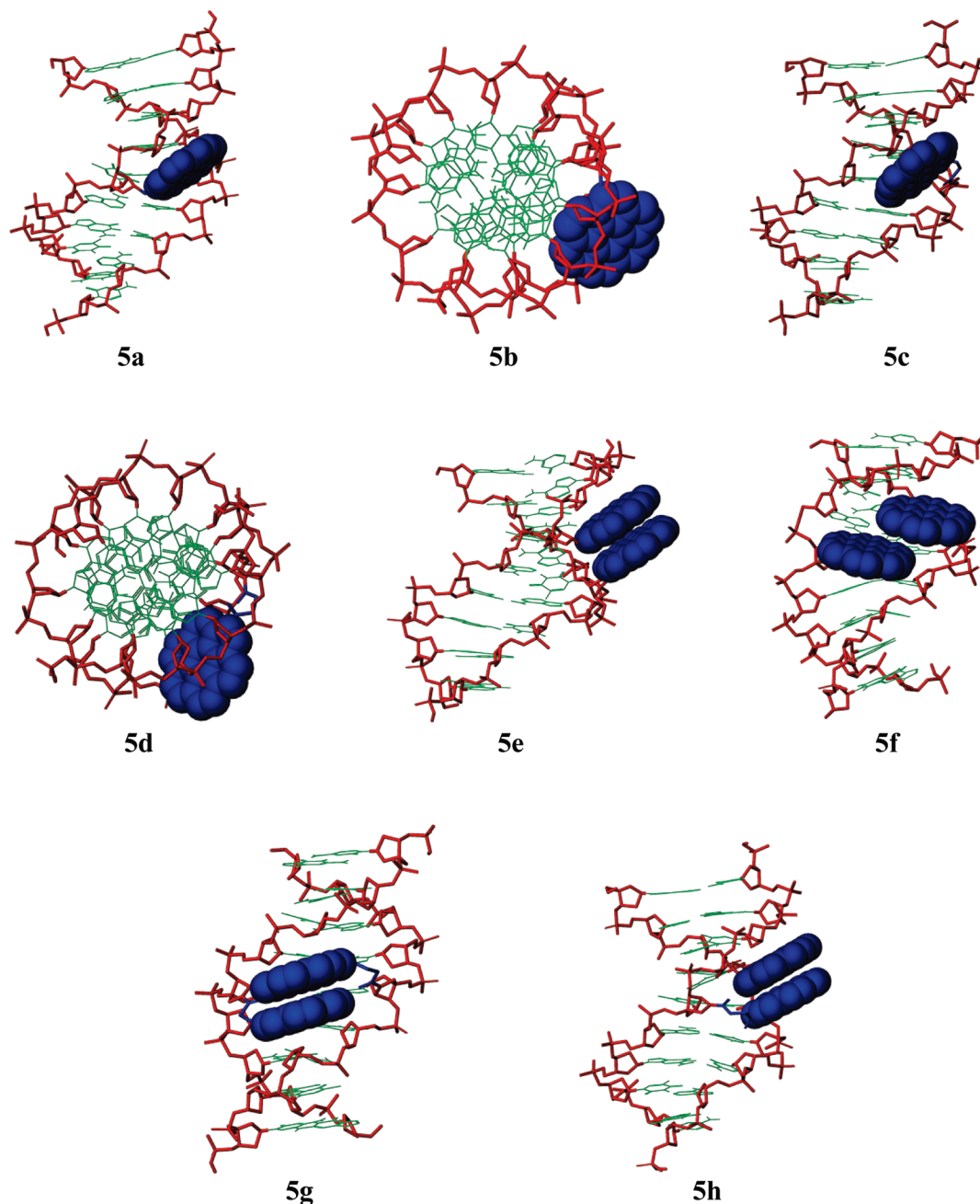


Figure 5. Energy-minimized structures of duplexes. (5a) ON3:DNA (monomer X in side view); (5b) ON3:DNA (monomer X in top view); (5c) ON7:DNA (monomer Y in side view); (5d) ON7:DNA (monomer Y in top view); (5e) ON3:ON4 (monomer X, “-1 zipper” arrangement); (5f) ON3:ON5 (monomer X, “+1 zipper” arrangement); (5g) ON7:ON8 (monomer Y, “-1 zipper” arrangement); and (5h) ON7:ON9 (monomer Y, “+1 zipper” arrangement) in side view. Color code: Sugar phosphate backbone (red); coronene (blue); nucleobases (green).

RNA complements showed a slight shift in emission maxima (~ 4 nm) to shorter wavelengths with a weakly increased fluorescence intensity (~ 1.5 -fold) (see ESI S4.10).

Incorporation of a single Y monomer in ONs (ON7–ON10) thus results in a broad, unstructured band with fluorescence emission maxima at ~ 453 nm, which is 51 nm red-shifted relative to pyrenecarbonyl-2'-amino-LNA ONs (18), 37 nm blue-shifted relative to perylene-3-carbonyl-2'-amino-LNA ONs (52), and 7–23 nm blue-shifted relative to (phenylethynyl)pyrenecarbonyl-2'-amino-LNA ONs (53). No characteristic changes in the shape of the spectral curves were observed.

Next, fluorescence properties of duplexes formed by ON3/ON7 and singly mismatched DNA/RNA targets were investigated. Noteworthy, as mentioned earlier, the mismatched duplexes display T_m values of more than 19 and 30 °C for ON3 and ON7, respectively. The resulting fluorescence spectra

(recorded at 10 °C) are shown in the electronic Supporting Information (Figures S4.1, S4.2, S4.6, and S4.7). Probe ON3 was seen to be equally sensitive to the presence of mismatched nucleosides in DNA and RNA targets with a ~ 2 -fold increase in fluorescence intensity for all singly mismatched complexes (Supporting Information Figures S4.1–S4.2). For probe ON7 containing a single monomer Y, the fluorescence effect of mismatches relative to the single-stranded ON7 and fully matched duplexes did not allow straightforward detection of mismatches (Supporting Information Figures S4.6–S4.7).

All duplexes having monomers X in both complementary strands displayed an unstructured emission band at $\lambda_{em} \sim 430$ nm. The fluorescence intensity of the “zippers” was lower in “-1 zipper” constitution and slightly higher in “+1 zipper” constitution than of the previously described duplexes having coronene monomer X in only one strand (Figure 3). Duplexes

having monomer **Y** in both complementary strands displayed an unstructured emission band at $\lambda_{em} \sim 484$ nm. In contrast, the fluorescence intensity of the “zipper” was higher in “-1 zipper” constitution and lower in “+1 zipper” constitution than of the previously described duplexes having coronene monomer **Y** in only one strand (Figure 4). Excimer emission was observed neither in single-stranded ONs (**ON3**–**ON10**) nor in their duplexes with DNA/RNA complements, whereas microcrystals of coronene showed both monomer and excimer emission bands (60). In contrast, insertion of pyrene-functionalized LNAs in “-1 zipper” motif resulted in strong excimer formation combined with increased thermal stability (15, 53).

Molecular modeling of duplexes formed between **ON3** (containing monomer **X**) or **ON7** (containing monomer **Y**) and cDNA (**ON2**) was performed using the AMBER force field (61, 62) as implemented in *MacroModel v 8.5* (63). Interstrand zipper arrangement modeling were also performed using the same method. All 9-mer duplexes were constructed with the coronene moiety of monomers **X** and **Y** in an extrahelical position. The observed low-energy structures were used for molecular dynamics simulations.

The model structure of the **ON3:ON2** hybrid suggests that the attachment of the methylcoronene moiety at the 2'-nitrogen atom of 2'-amino-LNA does not induce significant changes in the duplex geometry and that coronene binds in the minor groove without stacking with the nucleobases (Figure 5a,b). On the other hand, the model structure of hybrid **ON7:ON2** revealed many low-energy conformations during dynamics. This can be explained by the more flexible nature of the 4-oxobutanoyl linker of monomer **Y** though the coronene moiety shown still to be positioned in the minor groove (Figure 5c,d). Modeling results of zipper hybrid **ON3:ON4** showed the two coronene moieties to be stacking while being positioned in the minor groove (Figure 5e), which could explain the high T_m value measured for this “-1 zipper” duplex. This is substantiated for the **ON3:ON5** hybrid in which the two coronene moieties only partially stack (Figure 5f), thus offering an explanation of the lower T_m value observed in this case. The model structure of hybrid **ON7:ON8** showed the closest arrangement of the two coronene moieties stacking with each other and with nucleobases (Figure 5g), which correlates with the very high T_m value measured. Hybrid **ON7:ON9** showed the two coronene moieties to nicely stack in the minor groove (Figure 5h), but without stacking with the nucleobases.

CONCLUSION

We have studied hybridization and fluorescence properties of coronene moieties attached to the N2-nitrogen atom of 2'-amino-LNA. Incorporation of a single **X** monomer containing a methylcoronene moiety attached to 2'-amino-LNA induced increased T_m values (up to 3 °C) together with quenching of fluorescence intensity when bound to cDNA/RNA. Interestingly, upon incorporation of two **X** monomers separated by one nucleotide in a short ON, a 2-fold increase in fluorescence intensity of the resulting duplex with cDNA was observed. Additionally, significant mismatch discrimination was observed by fluorescence changes when a single monomer **X** was incorporated into an ON. Incorporation of monomer **Y** containing an oxobutanoylcoronene moiety attached to 2'-amino-LNA led to remarkably increased thermal affinity toward DNA/RNA complements (up to 15 °C per modification) together with a bathochromic shift in UV absorption upon hybridization with cDNA/RNA. No specific difference in fluorescence intensity was observed by hybridization upon incorporation of two **Y** monomers into a short ON. Interestingly, incorporation of a single monomer **Y** into a short ON allowed better mismatch discrimination toward RNA compared to DNA. The fluorescence

properties of the coronene-modified ONs introduced herein, such as fluorescence induced mismatch discrimination and a bathochromic shift in UV absorption upon hybridization with cDNA/RNA, testify to a significant potential for applications in nucleic acid based diagnostics.

ACKNOWLEDGMENT

The Nucleic Acid Center is a research center of excellence funded by the Danish National Research Foundation. We thank the Danish National Research Foundation for financial support.

Note Added after ASAP Publication: Due to a production error, an uncorrected version of this paper was inadvertently published on Jan 25, 2010. The corrected version was reposted on Feb 3, 2010.

Supporting Information Available: Steady-state fluorescence studies of ONs; protocol for molecular modeling studies; absorption and emission maxima of ONs; steady-state fluorescence emission spectras; An illustrative example of thermal denaturation curve and ^1H NMR spectra of **2a** and **2b**. This material is available free of charge via the Internet at <http://pubs.acs.org>.

LITERATURE CITED

- (1) Ranasinghe, R. T., and Brown, T. (2005) Fluorescence based strategies for genetic analysis. *Chem. Commun.* 5487–5502.
- (2) Tyagi, S., and Kramer, F. R. (1996) Molecular beacons: Probes that fluoresce upon hybridization. *Nat. Biotechnol.* 14, 303–308.
- (3) Seo, Y. J., Ryu, J. H., and Kim, B. H. (2005) Quencher-free, end-stacking oligonucleotides for probing single-base mismatches in DNA. *Org. Lett.* 7, 4931–4933.
- (4) Marx, A., and Seitz, O. (2008) *Methods in Molecular Biology* Vol. 429, *Molecular Beacons: Signalling Nucleic Acid Probes*, Humana Press, Totowa, NJ.
- (5) Kodama, S., Asano, S., Moriguchi, T., Sawai, H., and Shinzuka, K. (2006) Novel fluorescent oligo DNA probe bearing a multi-conjugated nucleoside with a fluorophore and a non-fluorescent intercalator as a quencher. *Bioorg. Med. Chem. Lett.* 16, 2685–2688.
- (6) Whitcombe, D., Theaker, J., Guy, S. P., Brown, T., and Little, S. (1999) Detection of PCR products using self-probing amplicons and fluorescence. *Nat. Biotechnol.* 17, 804–807.
- (7) Holland, P. M., Abramson, R. D., Watson, R., and Gelfand, D. H. (1991) Detection of specific polymerase chain reaction product by utilizing the 5'-3' exonuclease activity of *Thermus aquaticus* DNA polymerase. *Proc. Natl. Acad. Sci. U.S.A.* 88, 7276–7280.
- (8) Nazarenko, I. A., Bhatnagar, S. K., and Hohman, R. J. (1997) A closed tube format for amplification and detection of DNA based on energy transfer. *Nucleic Acids Res.* 25, 2516–2521.
- (9) Yamana, K., Gokota, T., Ozaki, H., Nakono, H., Sengen, O., and Shimidzu, T. (1992) Enhanced fluorescence in the binding of oligonucleotides with a pyrene group in the sugar fragment to complementary polynucleotides. *Nucleosides Nucleotides* 11, 383–390.
- (10) Lewis, F. D., Zhang, Y., and Letsinger, R. L. (1997) Bispirenyl excimer fluorescence: A sensitive oligonucleotide probe. *J. Am. Chem. Soc.* 119, 5451–5452.
- (11) Kostenko, E., Dobrikov, M., Pyshnyi, D., Petyuk, V., Komarova, N., Vlassov, V., and Zenkova, M. (2001) 5'-Bis-pyrenylated oligonucleotides displaying excimer fluorescence provide sensitive probes of RNA sequence and structure. *Nucleic Acids Res.* 29, 3611–3620.
- (12) Yamana, K., Ohtani, Y., Nakano, H., and Saito, I. (2003) Bispirenyl labeled DNA aptamer as an intelligent fluorescent biosensor. *Bioorg. Med. Chem. Lett.* 13, 3429–3431.
- (13) Dioubankova, N. N., Malakhov, A. D., Stetsenko, D. A., Gait, M. J., Volynsky, P. E., Efremov, R. G., and Korshun, V. A. (2003) Pyrenemethyl *ara*-uridine-2'-carbamate: a strong inter-

- strand excimer in the major groove of a DNA duplex. *Chem-BioChem* 4, 841–847.
- (14) Okamoto, A., Ichiba, T., and Saito, I. (2004) Pyrene-labeled oligodeoxynucleotide probe for detecting base insertion by excimer fluorescence emission. *J. Am. Chem. Soc.* 126, 8364–8365.
- (15) Hrdlicka, P. J., Babu, B. R., Sørensen, M. D., and Wengel, J. (2004) Interstrand communication between 2'-N-(pyren-1-yl)-methyl-2'-amino-LNA monomers in nucleic acid duplexes: directional control and signalling of full complementarity. *Chem. Commun.* 1478–1479.
- (16) Kawai, K., Yoshida, H., Takada, T., Tojo, S., and Majima, T. (2004) Formation of pyrene dimer radical cation at the internal site of oligodeoxynucleotides. *J. Phys. Chem. B* 108, 13547–13550.
- (17) Okamoto, A., Kanatani, K., and Saito, I. (2004) Pyrene-labeled base-discriminating fluorescent DNA probes for homogeneous SNP typing. *J. Am. Chem. Soc.* 126, 4820–4827.
- (18) Hrdlicka, P. J., Babu, B. R., Sørensen, M. D., Harrit, N., and Wengel, J. (2005) Multilabeled pyrene-functionalized 2'-amino-LNA probes for nucleic acid detection in homogeneous fluorescence assays. *J. Am. Chem. Soc.* 127, 13293–13299.
- (19) Nakamura, M., Fukunaga, Y., Sasa, K., Ohtoshi, Y., Kanaori, K., Hayashi, H., Nakano, H., and Yamana, K. (2005) Pyrene is highly emissive when attached to the RNA duplex but not to the DNA duplex: the structural basis of this difference. *Nucleic Acids Res.* 33, 5887–5895.
- (20) Novopashina, D. S., Stetsenko, D. A., Totskaya, O. S., Repkova, M. N., and Venyaminova, A. G. (2005) 2'-Bis-pyrene modified oligonucleotides: sensitive fluorescent probes of nucleic acids structure. *Nucleosides Nucleotides Nucleic Acids* 24, 729–734.
- (21) Yamana, K., Fukunaga, Y., Ohtani, Y., Sato, S., Nakamura, M., Kim, W. J., Akaike, T., and Maruyama, A. (2005) DNA mismatch detection using a pyrene-excimer-forming probe. *Chem. Commun.* 2509–2511.
- (22) Hrdlicka, P. J., Kumar, T. S., and Wengel, J. (2005) Targeting of mixed sequence double-stranded DNA using pyrene-functionalized 2'-amino- α -L-LNA. *Chem. Commun.* 4279–4281.
- (23) Dohno, C., and Saito, I. (2005) Discrimination of single nucleotide alterations by G-specific fluorescence quenching. *ChemBioChem* 6, 1075–1081.
- (24) Honcharenko, D., Zhou, C., and Chattopadhyaya, J. (2008) Modulation of pyrene fluorescence in DNA probes depends upon the nature of the conformationally restricted nucleotide. *J. Org. Chem.* 73, 2829–2842.
- (25) Didenko, V. V. (2006) *Methods in Molecular Biology Vol. 335, Fluorescent Energy Transfer Nucleic Acid Probes*, Humana Press, Totowa, NJ.
- (26) Marras, S. A. E., Tyagi, S., and Kramer, F. R. (2006) Real-time assays with molecular beacons and other fluorescent nucleic acid hybridization probes. *Clin. Chim. Acta* 363, 48–60.
- (27) French, D. J., Archard, C. L., Brown, T., and McDowell, D. G. (2001) HyBeacon™ probes: a new tool for DNA sequence detection and allele discrimination. *Mol. Cell. Probes* 15, 363–374.
- (28) Crockett, A. O., and Wittwer, C. T. (2001) Fluorescein-labeled oligonucleotides for real-time PCR: using the inherent quenching of deoxyguanosine nucleotides. *Anal. Biochem.* 290, 89–97.
- (29) Yamana, K., Zako, H., Asazuma, K., Iwase, R., Nakano, H., and Murakami, A. (2001) Fluorescence detection of specific RNA sequences using 2'-pyrene-modified oligonucleotides. *Angew. Chem., Int. Ed. Engl.* 40, 1104–1106.
- (30) French, D. J., Archard, C. L., Andersen, M. T., and McDowell, D. G. (2002) Ultra-rapid DNA analysis using HyBeacon™ probes and direct PCR amplification from saliva. *Mol. Cell. Probes* 16, 319–326.
- (31) Yamana, K., Iwai, T., Ohtani, Y., Sato, S., Nakamura, M., and Nakano, H. (2002) Bis-pyrene-labeled oligonucleotides: sequence specificity of excimer and monomer fluorescence changes upon hybridization with DNA. *Bioconjugate Chem.* 13, 1266–1273.
- (32) Korshun, V. A., Stetsenko, D. A., and Gait, M. J. (2002) Novel uridin-2'-yl carbamates: synthesis, incorporation into oligodeoxyribonucleotides, and remarkable fluorescence properties of 2'-pyren-1-ylmethylcarbamate. *J. Chem. Soc., Perkin Trans. I*, 1092–1104.
- (33) Mahara, A., Iwase, R., Sakamoto, T., Yamana, K., Yamaoka, T., and Murakami, A. (2002) Bispyrene-conjugated 2'-O-methyloligonucleotide as a highly specific RNA-recognition probe. *Angew. Chem., Int. Ed.* 41, 3648–3650.
- (34) Dobson, N., McDowell, D. G., French, D. J., Brown, L. J., Mellor, J. M., and Brown, T. (2003) Synthesis of HyBeacons and dual-labelled probes containing 2'-fluorescent groups for use in genetic analysis. *Chem. Commun.* 1234–1235.
- (35) Vaughn, C. P., and Elenitoba-Johnson, K. S. J. (2003) Hybridization-induced dequenching of fluorescein-labeled oligonucleotides: a novel strategy for PCR detection and genotyping. *Am. J. Pathol.* 163, 29–35.
- (36) Leijon, M., Mousavi-Jazi, M., and Kubista, M. (2006) LightUp probes in clinical diagnostics. *Mol. Asp. Med.* 27, 160–175.
- (37) Singh, S. K., Nielsen, P., Koshkin, A. A., and Wengel, J. (1998) LNA (locked nucleic acids): synthesis and high-affinity nucleic acid recognition. *Chem. Commun.* 455–456.
- (38) Obika, S., Nanbu, D., Hari, Y., Andoh, J., Morio, K., Doi, T., and Imanishi, T. (1998) Stability and structural features of the duplexes containing nucleoside analogues with a fixed N-type conformation, 2'-O,4'-C-methyleneribonucleosides. *Tetrahedron Lett.* 39, 5401–5404.
- (39) Koshkin, A. A., Singh, S. K., Nielsen, P., Rajwanshi, V. K., Kumar, R., Meldgaard, M., Olsen, C. E., and Wengel, J. (1998) LNA (Locked Nucleic Acids): Synthesis of the adenine, cytosine, guanine, 5-methylcytosine, thymine and uracil bicyclonucleoside monomers, oligomerisation, and unprecedented nucleic acid recognition. *Tetrahedron* 54, 3607–3630.
- (40) Koshkin, A. A., Nielsen, P., Meldgaard, M., Rajwanshi, V. K., Singh, S. K., and Wengel, J. (1998) LNA (Locked Nucleic Acid): An RNA mimic forming exceedingly stable LNA:LNA duplexes. *J. Am. Chem. Soc.* 120, 13252–13253.
- (41) Wengel, J. (1999) Synthesis of 3'-C- and 4'-C-branched oligodeoxynucleotides and the development of Locked Nucleic Acid (LNA). *Acc. Chem. Res.* 32, 301–310.
- (42) Bondensgaard, K., Petersen, M., Singh, S. K., Rajwanshi, V. K., Kumar, R., Wengel, J., and Jacobsen, J. P. (2000) Structural studies of LNA:RNA duplexes by NMR: conformations and implications for RNase H activity. *Chem.—Eur. J.* 6, 2687–2695.
- (43) Singh, S. K., Kumar, R., and Wengel, J. (1998) Synthesis of 2'-amino-LNA: A novel conformationally restricted high-affinity oligonucleotide analogue with a handle. *J. Org. Chem.* 63, 10035–10039.
- (44) Babu, B. R., Hrdlicka, P. J., McKenzie, C. J., and Wengel, J. (2005) Optimized DNA targeting using N,N-bis(2-pyridylmethyl)- β -alanyl-2'-amino-LNA. *Chem. Commun.* 1705–1707.
- (45) Højland, T., Kumar, S., Babu, B. R., Umamoto, T., Albæk, N., Sharma, P. K., Nielsen, P., and Wengel, J. (2007) LNA (locked nucleic acid) and analogs as triplex-forming oligonucleotides. *Org. Biomol. Chem.* 5, 2375–2379.
- (46) Sørensen, M. D., Kværnø, L., Bryld, T., Hakansson, A. E., Verbeure, B., Gaubert, G., Herdewijn, P., and Wengel, J. (2002) α -L-ribo-configured Locked Nucleic Acid (r-L-LNA): Synthesis and properties. *J. Am. Chem. Soc.* 124, 2164–2176.
- (47) Petersen, M., and Wengel, J. (2003) LNA: a versatile tool for therapeutics and genomics. *Trends Biotechnol.* 21, 74–81.
- (48) Elmén, J., Lindow, M., Schütz, S., Lawrence, M., Petri, A., Obad, S., Lindholm, M., Hedtjærn, M., Hansen, H. F., Berger, U., Gullans, S., Kearney, P., Sarnow, P., Straarup, E. M., and Kauppinen, S. (2008) LNA-mediated microRNA silencing in non-human primates. *Nature* 452, 896–899.
- (49) Sørensen, M. D., Petersen, M., and Wengel, J. (2003) Functionalized LNA (locked nucleic acid): high-affinity hybridization of oligonucleotides containing N-acylated and N-alkylated 2'-amino-LNA monomers. *Chem. Commun.* 2130–2131.

- (50) Kumar, T. S., Wengel, J., and Hrdlicka, P. J. (2007) 2'-N-(Pyren-1-yl)acetyl-2'-Amino- α -L-LNA: Synthesis and detection of single nucleotide mismatches in DNA and RNA targets. *ChemBioChem* 8, 1122–1125.
- (51) Lindegaard, D., Madsen, A. S., Astakhova, I. V., Malakhov, A. D., Babu, B. R., Korshun, V. A., and Wengel, J. (2008) Pyrene-perylene as a FRET pair coupled to the N2'-functionality of 2'-amino-LNA. *Bioorg. Med. Chem.* 16, 94–99.
- (52) Astakhova, I. V., Korshun, V. A., Jahn, K., Kjems, J., and Wengel, J. (2008) Perylene attached to 2'-amino-LNA: synthesis, incorporation into oligonucleotides, and remarkable fluorescence properties *in vitro* and in cell culture. *Bioconjugate Chem.* 19, 1995–2007.
- (53) Astakhova, I. V., Korshun, V. A., and Wengel, J. (2008) Highly fluorescent conjugated pyrenes in nucleic acid probes: (phenylethynyl)pyrenecarbonyl-functionalized Locked Nucleic Acids. *Chem.—Eur. J.* 14, 11010–11026.
- (54) Nijegorodov, N., Mabbs, R., and Downey, W. S. (2001) Evolution of absorption, fluorescence, laser and chemical properties in the series of compounds perylene, benzo(ghi) perylene and coronene. *Spectrochim. Acta, Part A* 57, 2673–2685.
- (55) Davenport, L., Shen, B., Joseph, T. W., and Straher, M. P. (2001) A novel fluorescent coronenyl-phospholipid analogue for investigations of submicrosecond lipid fluctuations. *Chem. Phys. Lipids* 109, 145–156.
- (56) Nagata, C., Kodama, M., Tagashira, Y., and Imamura, A. (1966) Interaction of polynuclear aromatic hydrocarbons, 4-nitroquinoline 1-oxides, and various dyes with DNA. *Biopolymers* 4, 409–427.
- (57) Zinger, D., and Geacintov, N. E. (1988) Acrylamide and molecular oxygen fluorescence quenching as a probe of solvent-accessibility of aromatic fluorophores complexed with DNA in relation to their conformations: coronene-DNA and other complexes. *Photochem. Photobiol.* 47, 181–188.
- (58) Rosenbohm, C., Christensen, S. M., Sørensen, M. D., Pedersen, D. S., Larsen, L.-E., Wengel, J., and Koch, T. (2003) Synthesis of 2'-amino-LNA: a new strategy. *Org. Biomol. Chem.* 1, 655–663.
- (59) Woods, K. K., Maehigashi, T., Howerton, S. B., Sines, S. B., Sines, C. C., Tannenbaum, S., and Williams, L. D. (2004) High-resolution structure of an extended A-tract: [d(CGCAAATTTGCG)]₂. *J. Am. Chem. Soc.* 126, 15330–15331.
- (60) Seko, T., Ogura, K., Kawakami, Y. Y., Sugino, H., Toyotama, H., and Tanaka, J. (1998) Excimer emission of anthracene, perylene, coronene and pyrene microcrystals dispersed in water. *Chem. Phys. Lett.* 291, 438–444.
- (61) Weiner, S. J., Kollman, P. A., Case, D. A., Singh, U. C., Ghio, C., Alagona, G., Profeta, S., and Weiner, P. (1984) A new force field for molecular mechanical simulation of nucleic acids and proteins. *J. Am. Chem. Soc.* 106, 765–784.
- (62) Weiner, S. J., Kollman, P. A., Nguyen, D. T., and Case, D. A. (1986) An all atom force field for simulations of proteins and nucleic acids. *J. Comput. Chem.* 7, 230–252.
- (63) *MacroModel v 8.5*, Schrödinger, LLC, New York, 2007. BC900421R